Optimization of a 42.7 Gb/s wavelength tunable RZ transmitter using a linear spectrogram technique

Robert Maher,[1,*] Prince M. Anandarajah,[1] Andrew D. Ellis,[2] Douglas Reid,[1] and Liam P. Barry[1]

[1]*Research Institute for Networks and Communications Engineering, Dublin City University, Glasnevin, Dublin 9, Ireland*

[2]*Photonics Systems Group, Tyndall National Institute, Lee Maltings Complex, Prospect Row, Cork, Ireland*

[*]*Corresponding author: robert.maher@eeng.dcu.ie*

Abstract: The optimization of a wavelength tunable RZ transmitter, consisting of an electro-absorption modulator and a SG DBR tunable laser, is carried out using a linear spectrogram based characterization and leads to 1500 km transmission at 42.7 Gb/s independent of the operating wavelength. We demonstrate that, to ensure optimum and consistent transmission performance over a portion of the C-band, the RF drive and bias conditions of the EAM must be varied at each wavelength. The sign and magnitude of the pulse chirp (characterized using the linear spectrographic technique) is therefore tailored to suit the dispersion map of the transmission link. Results achieved show that by optimizing the drive and DC bias applied to the EAM, consistent transmission performance can be achieved over a wide wavelength range. Failure to optimize the EAM drive conditions at each wavelength can lead to serious degradation in system performance.

OCIS codes: (060.0060) Fiber optics and optical communications; (060.5530) Pulse propagation and temporal solitons.

References and links

1. B. Mikkelsen, C. Rasmussen, P. Mamyshev, F. Liu, S. Dey and F. Rosca, "Deployment of 40 Gb/s Systems: Technical and Cost Issues," in Optical Fiber Communications Conference and Exposition and The National Fiber Optic Engineers Conference on CD-ROM (Optical Society of America, Los Angeles, CA, 2004), ThE6.
2. A. Sano and Y. Miyamoto, "Technologies for Ultrahigh Bit-Rate WDM Technologies," in Laser and Electro-Optics Society Annual Metting, pp. 290-291 (2007).
3. R. Ludwig, U. Feiste, E. Dietrich, H.G. Weber, D. Breuer, M. Martin and F. Kuppers, "Experimental Comparison of 40 Gb/s RZ and NRZ Transmission over Standard Singlemode Fiber," Electron. Lett. **35**, 2216-2218 (1999).
4. B. Konrad, K. Petermann, J. Berger, R. Ludwig, C.M. Weinert, H.G. Weber and B. Schmauss, "Impact of Fiber Chromatic Dispersion in High-Speed TDM Transmission Systems," IEEE J. Lightwave. Technol. **20**, 2129-2135 (2002).
5. N. Madamopoulos, D.C. Friedman, I. Tomkos and A. Boskovic, "Study of the Performance of a Transparent and Reconfigurable Metropolitan Area Network," IEEE J. Lightwave. Technol. **20**, 937-945 (2002).
6. M. Chen, Y. Shi, C. Qiu, H. Chen and S. Xie, "Residual Chromatic-Dispersion Monitoring and Dynamic Compensation in 40 Gb/s Systems," IEEE Photon. Technol. Lett. **19**, 1142-1144 (2007).
7. P.J. Winzer and R.J. Essiambre, "Electronic pre-Distortion for Advanced Modulation Formats," in Optical Fiber Communications Conference and Exposition and The National Fiber Optic Engineers Conference on CD-ROM (Optical Society of America, Los Angeles, CA, 2005), Tu4.4.2.
8. E. Yamada, T. Imai, T. Komukai and M. Nakazawa, "10 Gb/s Soliton Transmission over 2900km of using 1.3µm Singlemode Fibers and Dispersion Compensation using Chirped Fiber Bragg Gratings," Electron. Lett. **35**, 728-729 (1999).
9. B. Bakhshi, M. Vaa, E.A. Golovchenko, W.W. Patterson, R.L. Maybach and N.S. Bergano, "Comparison of CRZ, RZ and NRZ Modulation Formats in a 64 x x12.3 Gb/s WDM Transmission Experiment over 9000

#95692 - $15.00 USD Received 1 May 2008; revised 19 Jun 2008; accepted 19 Jun 2008; published 11 Jul 2008

km," in Optical Fiber Communications Conference and Exposition and The National Fiber Optic Engineers Conference on CD-ROM (Optical Society of America, Los Angeles, CA, 2001), WF4-1.
10. D.C. Zhang, X.L. Li, X.R. Zhang, J.H. Li, A.S. Xu, Z.y. Wang, H.B. Li, Z.B. Li, F. Zhang and Z.Y. Chen, "42.8 Gb/s Electro-Absorption Modulated NRZ Transmission over 1200 km Standard Singlemode Fiber," Electron. Lett. **43**, 237-239 (2007).
11. L.A. Coldren, G. Fish, Y. Akulova, J.S. Barton, L. Johansson and C.W. Coldren, "Tunable Semiconductor Lasers: A Tutorial," IEEE J. Lightwave. Technol. **22**, 193-202 (2004).
12. P.C. Koh, C. Schow, Y.A. Akulova and G.A. Fish, "Correlation Between Dispersion Penalty and Time-Resolved Chirp for an Integrated Widely Tunable Electroabsorption-Modulated SGDBR Laser Across the EDFA Gain Bandwidth," IEEE Photon. Technol. Lett. **15**, 1011-1013 (2003).
13. S. Makino, K. Shinoda, T. Shiota, T. Kitatani, S. Tanaka and M. Aoki, "10Gb/s – 80 km Transmisiso by 100 GHz-Spacing, 8-Channel Wavelength-Tunable 1.55 μm InGaAlAs Electro-Absorption Modulator Integrated DFB Laser," in Optical Fiber Communications Conference and Exposition and The National Fiber Optic Engineers Conference on CD-ROM (Optical Society of America, San Diego, CA, 2008), OThK4.
14. R. Maher, P.M. Anandarajah and L.P. Barry, "Optimized Performance Map of an EAM for Pulse Generation and Demultiplexing via FROG Characterization," J. Opt. Commun. **273**, 500-505 (2007).
15. J.W. Raring, L.A. Johansson, E.J. Skogen, M.N. Sysak, H.N. Poulsen, S.P. DenBaars and L.A. Coldren, "40-Gb/s Widely Tunable Low-Drive-Voltage Electroabsorption-Modulated Transmitters," IEEE J. Lightwave. Technol. **25**, 239-248 (2007).
16. C. Dorrer and I. Kang, "Real-Time Implementation of Linear Spectrograms for the Characterization of High Bit-Rate optical Pulse Trains," IEEE Photon. Technol. Lett. **16**, 858-860 (2004).
17. C. Dorrer and I. Kang, "Simultaneous temporal characterization of telecommunication optical pulses and modulators by use of spectrograms," OSA Opt. Lett. **27**, 1315-1317 (2002).
18. P.J. Winzer, C. Dorrer, R.J. Essiambre and I. Kang, "Chirped Return-to-Zero Modulation by Imbalanced Pulse Carver Driving Signals," IEEE Photon. Technol. Lett. **16**, 1379-1381 (2004).
19. B.C. Thomsen, M.A.F. Roelens, R.T. Watts and D.J. Richardson, "Comparison Between Nonlinear and Linear Spectrographic Techniques for the Complete Characterization of High Bit-Rate Pulses used in Optical Communications," IEEE Photon. Technol. Lett. **17**, 1914-1916 (2005).
20. D.J. Kane, "Real-Time Measurement of Ultrashort Laser Pulses Using Principle Component Generalized Projections," IEEE J. Sel. Topics. in Quant. Electron. **4**, 278-284 (1998).
21. T. Widdowson and A.D. Ellis, "20 Gbit/s Soliton Transmission over 125 Mm," Electron. Lett. **30**, 1866-1868 (1994).
22. J.C. Cartledge and B. Christensen, "Optimum Operating Points for Electroabsorption Modulators in 10 Gb/s Transmission Sytems Using Dispersion Shifted Fiber," IEEE J. Lightwave. Technol. **16**, 349-357 (1998).
23. F. Devaux, Y. Sorel and F. Kerdiles, "Simple Measurement of Fiber Dispersion and of Chirp Parameter of Intensity Modulated Light Emitter," IEEE J. Lightwave. Technol. **11**, 1937-1940 (1993).
24. M. Suzuki and N. Edagawa and, "Dispersion Managed high-Capacity Ultra-Long-Haul Transmission," IEEE J. Lightwave. Technol. **21**, 916-928 (2003).

1. Introduction

Due to the continuous growth in IP data traffic, high-capacity and cost-efficient transmission systems are increasingly required for realizing future optical transport networks. As the next natural step in the data rate hierarchy, 40 Gb/s transmission has been the focus of extensive investigation in research and development for the past decade [1,2]. As optical systems move towards these higher data rates and also migrate from non-return-to-zero (NRZ) to return-to-zero (RZ) format (due to enhanced performance of RZ systems at 40 Gb/s and beyond) [3], the impact of chromatic dispersion in transmission fiber becomes more dramatic. Therefore, the use of dispersion management techniques and/or optical fiber non-linearity to counteract the dispersive effects must be precisely regulated [4]. An additional factor is the impact of component parameters, such as chirp, which also become more severe at data rates of 10 Gb/s and above, making impairment management a key aspect of modern transmission systems [5].

A major problem in long haul transmission systems is the variation of the residual dispersion associated with the dispersion map, which results in system performance degradation. Several dynamic dispersion compensation methods have been proposed to overcome the residual dispersion of a fiber optic link, but these schemes inevitably add extra cost and complexity to the system [6]. Alternatively, a pre-chirp can be applied to the generated pulses by employing dispersion compensating fiber (DCF), a phase modulator at the transmitter or electronic pre-distortion [7]. This could be used to counteract the residual

#95692 - $15.00 USD Received 1 May 2008; revised 19 Jun 2008; accepted 19 Jun 2008; published 11 Jul 2008

dispersion experienced through transmission over different wavelength channels, thus achieving greater transmission reach [8,9]. A simpler technique to optimize performance without additional hardware complexity makes use of the non-zero chirp value of the external modulator used to encode data onto the optical signal. In this case, the combined effect of the positive or negative chirp in the transmitter and the second-order dispersion provides a certain amount of compression after NRZ transmission, yielding enhanced performance for long haul transmission [10]. Therefore by accurately controlling the chirp of the generated pulses, a larger transmission distance may be achieved, while also ensuring an acceptable level of performance at all wavelengths.

Previous work in this area has mainly focused on dispersion limited NRZ transmission systems at data rates up to 40 Gb/s, where the EAM bias or RF drive voltage was adjusted to achieve uniform optical extinction over a wide wavelength range [11]. This technique has also been employed to maintain consistent NRZ transmission performance in monolithically integrated devices over a wide wavelength range at data rates of 2.5 and 10 Gb/s [12, 13]. However, for long distance RZ transmission systems using a dispersion managed transmission line, with negligible residual dispersion, it remains imperative to analyze the generated pulses in terms of pulse width (PW), extinction ratio (ER) and more importantly, the sign and magnitude of the pulse chirp. The non-optimization of these specific parameters at each operating wavelength, could lead to a large variation in transmission performance due to the interaction between these parameters and the non-linear response of the dispersion managed transmission line. The RZ wavelength tunable transmitter used for this work consisted of a sampled grating distributed Bragg reflector (SG DBR) tunable laser (TL) and an electro-absorption modulator (EAM). One of the main advantages of this technique is that the characteristics of the generated pulses (width, chirp and extinction ratio) can be varied by tuning the bias and drive conditions of the EAM [14]. The two components (TL and EAM) can also be easily integrated, therefore providing the potential for a low cost, small form factor and agile RZ tunable transmitter [15].

Performance analysis of the generated pulses in a 42.7 Gb/s transmission system, in terms of the transmission distance as a function of the input pulse characteristics, was carried out. The pulse width, chirp and extinction ratio of the tunable RZ transmitter were characterized using the linear spectrogram pulse characterization technique [16-18]. This technique has a very high sensitivity, is polarization insensitive and does not suffer from the temporal ambiguity in the measured fields that is associated with other measurement techniques, such as frequency resolved optical gating (FROG) [19]. By utilizing this measurement technique, an accurate performance map (in terms of PW, ER and Chirp) of the wavelength tunable transmitter, depending on RF drive and DC bias, could be constructed. Our transmission results show the importance of utilizing this map to tune the operating conditions of the EAM, to obtain an optimal RZ pulse that exhibits a chirp profile to match the residual dispersion that is experienced at each wavelength channel. This therefore reduces the cost of implementing per-channel dispersion compensating techniques and also extends the operating wavelength range of the SG DBR-EAM based transmitter. Operation of the EAM with a fixed bias and RF drive results in significant penalties, as regards the achievable error correctable transmission distance, as the operating wavelength of the transmitter is altered. We demonstrate for the first time that prior source characterization using a linear spectrographic technique allows the drive conditions of the modulator to be set, providing uniform transmission performance (1500 km) over a 20 nm wavelength range, with no external pre-chirping of the pulses. Furthermore, no pre or post-dispersion compensation techniques were employed in the transmission system.

2. Experimental setup

The linear spectrogram set-up used to perform the initial pulse characterization is depicted in Fig. 1. A 10 GHz clock signal (which was referenced to our pulse carving clock signal) passed through a phase shifter before being electrically multiplexed up to 40 GHz. This signal was then amplified and applied to a 40 GHz commercially available OKI EAM to perform the temporal gating. By using an EAM, the gate has the advantage of being polarization insensitive. The relative delay between the train of pulses and the gate was modified with the

#95692 - $15.00 USD Received 1 May 2008; revised 19 Jun 2008; accepted 19 Jun 2008; published 11 Jul 2008

voltage controlled phase shifter, which can introduce a delay sufficient enough to cover the 100 ps timing window. The spectrum of the pulse was recoded at each value of delay with an optical spectrum analyzer (OSA) which had a resolution of 0.01 nm. A computer was used to control the RF phase shifter and to record the spectra of the gated pulse, as a function of the delay between the pulse and the gate, to build up a spectrogram on a 128 x 128 grid. The intensity and phase of the generated pulses were then resolved by using a phase retrieval algorithm [20]. The generated pulses were characterized for a number of bias conditions (-1 to -2 V), a number of RF drive voltages (2.5 to 3.7 Vpp), and for three different wavelengths (1540.56, 1550.52 and 1560.20 nm). This characterization provided the chirp and temporal profile of the pulses, therefore giving an indication as to which drive conditions would produce similar pulse characteristics at each wavelength [14].

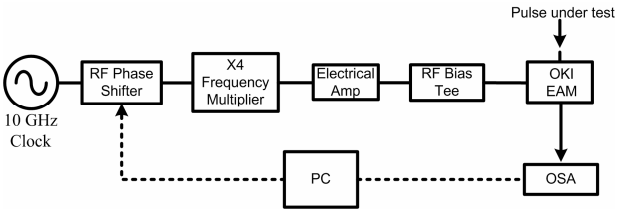

Fig. 1. 40 GHz linear spectrogram pulse measurement setup

Once the initial pulse characterization was complete, the 42.7 GHz pulse source was implemented in a re-circulating loop transmission system as depicted in Fig. 2. The pulse source consisted of a commercially available SG DBR tunable laser which provided the continuous wave light to a sinusoidally driven EAM. The EAM was a commercially available fiber-pigtailed InP modulator that operates over the entire C-band and has 10 InGaAs wells with InAlAs barriers. It was driven with a 42.7 GHz clock signal (40 GHz base rate with 7% overhead required for FEC) from a pulse pattern generator that passed through a phase shifter and a gain-controlled electrical amplifier. A 42.7 Gb/s NRZ pseudorandom binary sequence of length 2^7-1 (which was limited by our ability to generate a true 42.7 Gb/s PRBS bit signal) was used to modulate the pulse train with the aid of a mach-zehnder modulator (MZM) via a polarization controller (PC). The resultant STM-256 RZ signal was then passed through an EDFA operating in saturation and followed by a variable optical attenuator, to allow for an easily adjustable power level.

The transmission performance of the EAM-based pulse source was evaluated through a re-circulating loop. The loop had a round trip time of approximately 600 μs and consisted of two 50 km spans of SMF and two reels of DCF, approximately compensating for 40 and 60 km lengths respectively. The SMF exhibited a measured dispersion of 17.37 ps/nm.km and a specified dispersion slope of 0.06 ps/km/nm^2 at 1550 nm, while the slope-matched DCF had a dispersion of -99.3 ps/nm.km and a dispersion slope of -0.12 ps/km/nm^2 at 1550 nm. The calculated residual dispersion per loop was 4.3 ps/nm at 1550 nm, such that self phase modulation was required to balance a portion of the net residual dispersion. An average launch power of approximately 0 dBm remained constant as the operating wavelength was varied. Two EDFAs with 5.5 dB noise figures were used to overcome the accumulated attenuation of the fiber links whilst variable optical attenuators offered controllability over the power in the loop. An optical band pass filter (OBPF) with a 3 dB bandwidth of 2 nm was placed in the loop primarily to minimize the accumulation of out of band amplified spontaneous emission (ASE) but is also believed to have provided a degree of pulse reforming in combination with self phase modulation in the transmission fiber [21]. A PC was adjusted to maintain an optimum state of polarization by monitoring the BER performance. This optimization was carried out at each of the operating wavelengths and for each number of loop re-circulations. This optimization in effect, ensured that the impact of PMD was equalized (minimized) for all wavelengths.

#95692 - $15.00 USD Received 1 May 2008; revised 19 Jun 2008; accepted 19 Jun 2008; published 11 Jul 2008

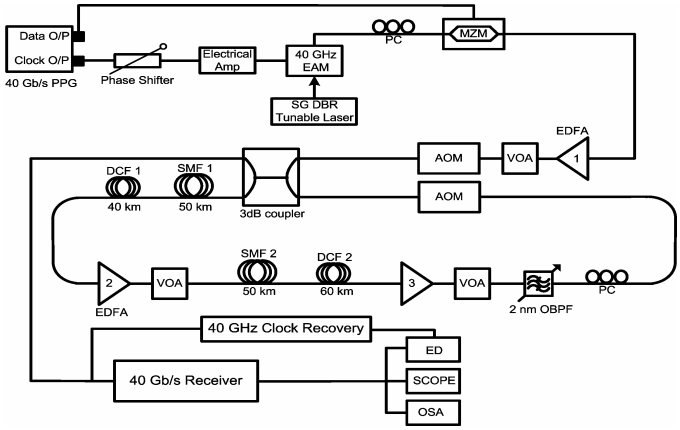

Fig. 2. 42.7 Gb/s transmission setup

The receiver consisted of two stages of optical amplification with each amplifier followed by an optical band pass filter to suppress ASE. Clock recovery was performed using a commercially available phase locked loop which was used to trigger the oscilloscope and error detector for eye and bit error rate (BER) analysis respectively. The BER was recorded as a function of the number of transmission loops, for each wavelength and drive condition of the tunable transmitter. An optical spectrum analyzer and a high speed oscilloscope were used to monitor the pulse spectrum and the received eyes respectively. All test equipment was gated using the loop timing signal to isolate the output after a given transmission distance.

3. Experimental results and discussion

Initially, the RZ wavelength tunable transmitter was employed in the re-circulating loop set-up at a wavelength of 1560.20 nm. The conditions allowing the greatest number of re-circulations within the FEC limit were obtained by tuning the DC bias of the EAM between -1.4 and -2 V in 0.2 V steps, and by tuning the peak-to-peak drive signal from 2.5 to 3.7 Vpp in 0.6 V steps. Once the greatest transmission distance was achieved, the bias, RF drive voltage and launch power (~ 0 dBm) were held constant and the operating wavelength was varied. Figure 3 represents this non-optimized scenario, where the RF drive (2.5 Vpp) and DC bias (-2 V) voltage applied to the EAM remained constant for each operating wavelength. The corresponding eye diagrams, recorded after 1000 km, are also illustrated in Fig. 3 (b). As can be seen, a great variability in transmission performance was obtained with the error correctable maximum distance (a BER of 10^{-3}) varying from 1000 to over 1500 km, or equivalently, the BER varying by over two orders of magnitude. Note that the slopes of the curves converge after 1200 km suggesting that a degree of soliton-like pulse stabilization occurs within the loop. At a BER of 10^{-4} (which is below the FEC limit to allow a slight margin for aging) a transmission distance of 1500 km was achieved when the tunable laser operated at channel 14 on the ITU grid (1560.20 nm), which decreased to 1000 km at 1540.56 nm (channel 64), representing a 33 percent drop in transmission performance. Such a large variance in system performance over a portion of the C-band wavelength range illustrates that constant EAM drive conditions, in the transmitter, will lead to unacceptable levels of performance over a wide wavelength range, which would be unacceptable in a real system.

Figure 4 illustrates the measured intensity and chirp profile of the pulses under the constant drive conditions (-2 V DC bias and 2.5 Vpp clock signal). The temporal widths of all three pulses are similar, having values of 4.9, 5.1 and 5.4 ps respectively. It is anticipated that such variations would result in a negligible impact on transmission performance, whilst the measured extinction ratio variation (25 to 31 dB) would also result in a negligible change in transmission distance. However, the chirp magnitude and more significantly the sign of the chirp varies significantly from one pulse to the other. At 1540.56 nm, where the greatest degradation in transmission performance was realized, the chirp profile is negative across the

#95692 - $15.00 USD Received 1 May 2008; revised 19 Jun 2008; accepted 19 Jun 2008; published 11 Jul 2008

centre of the pulse. At 1550.52 nm, the chirp profile flattens out and is slightly positive across the centre of the pulse with a decrease in magnitude [22]. Significantly, at 1560.20 nm, the sign of the chirp is opposite to that experienced at 1540.56 nm and there is a positive chirp profile. This profile best suits the given dispersion map of the transmission link, providing the greatest tolerance to the dispersive and non-linear effects experienced during transmission. By comparing the intensity and phase information of the generated pulses at each wavelength, with the reference wavelength (1560.20 nm), an estimate can be made as to which drive conditions for the transmitter would achieve a similar pulse profile at each wavelength, thereby achieving extended transmission distance and greater performance uniformity over the wavelength tuning range.

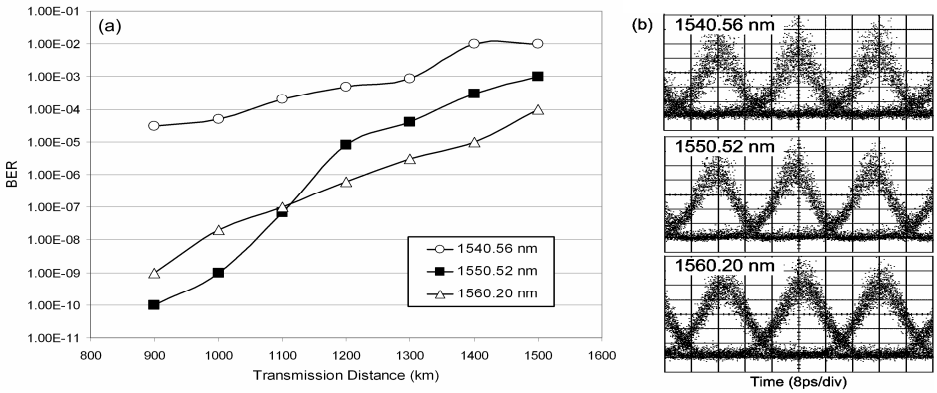

Fig. 3. (a). BER as a function of transmission distance for a non-optimized transmitter. (b). Corresponding eye diagrams received after 1000 km for 1540.56, 1550.52 and 1560.20 nm respectively.

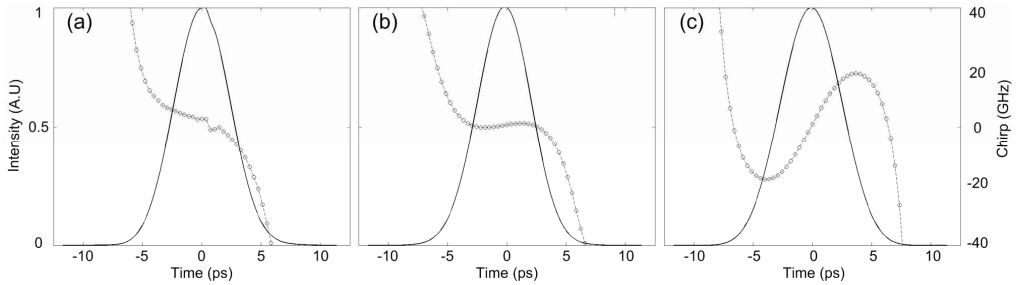

Fig. 4. Linear Spectrogram characterization of the non-optimized pulses with constant bias (-2 V) and an RF drive (2.5 Vpp) applied to the EAM; for the three different wavelengths, (a) 1540.56 nm, (b) 1550.52 nm and (c) 1560.20 nm. Intensity – solid line, Frequency Chirp – circled dotted line.

The differences in the chirp profiles between wavelengths are confirmed by considering the alpha parameter profile of the EAM as depicted in Fig. 5, which was recorded using the interferometric technique outlined by Devaux et al [23]. When the EAM is biased at -2 V, at a wavelength of 1540.56 nm, the alpha factor is negative (-0.6). As the RF drive voltage applied to the device is relatively low, the chirp profile remains negative in sign. Alternatively, when operating at 1560.20 nm, the alpha parameter crosses zero at a bias voltage of -1.8 V. Therefore, while biased at -2 V, the alpha factor will swing from a positive to a negative value due to the applied RF drive voltage, resulting in a positive chirp profile. In order to obtain similar transmission performance at 1540.56 nm, the bias of the EAM must be adjusted to -1.4 V and with an increased RF drive voltage of approximately 3.1 Vpp. Similarly, when operating at 1550.52 nm, the bias must be slightly reduced to approximately -1.8 V and again driven with a larger RF drive of 3.1 Vpp. The change in bias at this wavelength is not as large, as its alpha factor profile is closer to that of 1560.20 nm. The corresponding pulse and chirp

#95692 - $15.00 USD Received 1 May 2008; revised 19 Jun 2008; accepted 19 Jun 2008; published 11 Jul 2008

profiles at the new optimized EAM drive conditions for the three wavelengths are illustrated in Fig. 6. It is important to note however, that the alpha parameter profile is characterized under small signal analysis and will change under large signal modulation of the EAM. Therefore the additional information (chirp, sign and magnitude) provided by the linear spectrogram characterization, allows for a more consistent level of transmission performance for each particular EAM.

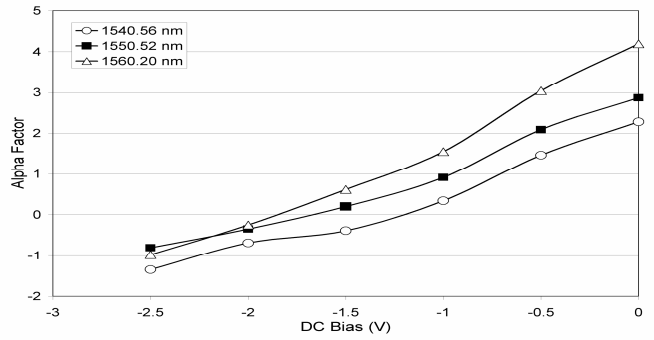

Fig. 5. Alpha Factor as a function of DC bias voltage for EAM at 1540.56, 1550.52 and 1560.20 nm

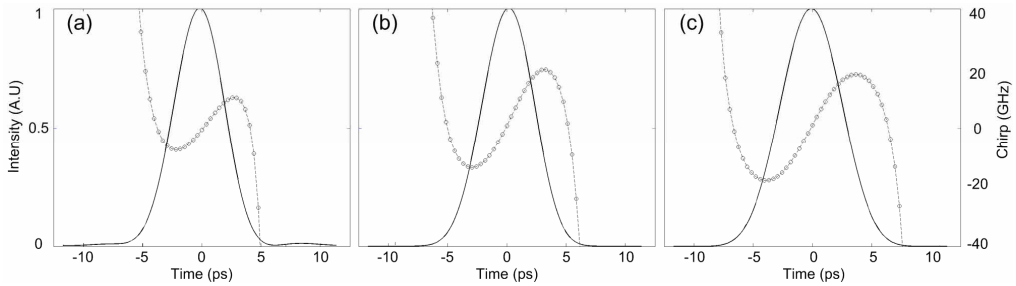

Fig. 6. Linear Spectrogram characterization of the optimized pulses for the three different wavelengths, (a) 1540.56 nm, (b) 1550.52 nm and (c) 1560.20 nm. Intensity – solid line, Frequency Chirp – circled dotted line.

The sign and magnitude of the pulse chirp profiles at all three wavelengths are now similar, therefore indicating that a more consistent level of performance may be achieved across the C-band. To verify this, the transmitter was again employed in the 42.7 Gb/s re-circulating transmission test bed to determine the performance of the optimized pulses at each wavelength. Figure 7 illustrates the BER performance as a function of transmission distance, with the corresponding eye diagrams, recorded after 1000 km of SMF. By optimizing the drive conditions of the EAM in our RZ tunable transmitter, a greater transmission distance (within an error correctable level) has been achieved at 1540.56 and 1550.52 nm. A distance of 1400 km at a BER of 10^{-4} was realized while operating at 1540.56 nm, representing an improvement of 400 km, relative to the non-optimized scenario. At 1550.52 nm, there is an improvement of 150 km (relative to its non-optimized case), thereby ensuring a near consistent level of performance over the entire wavelength range. Extrapolation suggests that the error correctable maximum distances below 10^{-3} were 1500, 1600 and 1600 km at the operating wavelengths of 1540.56, 1550.52 and 1560.20 nm respectfully. The corresponding OSA spectra for each wavelength, recorded after 1000 km, are shown in Fig. 8. In order to maximize the transmission distance of our optical RZ pulses, the OBPF in the re-circulating loop was slightly detuned (prior to transmitter optimization) from the carrier frequency, producing a vestigial side-band (VSB) RZ signal. This is a simple, low cost method employed to increase the spectral efficiency of the generated pulses, therefore improving their fiber dispersion tolerance [24].

#95692 - $15.00 USD Received 1 May 2008; revised 19 Jun 2008; accepted 19 Jun 2008; published 11 Jul 2008

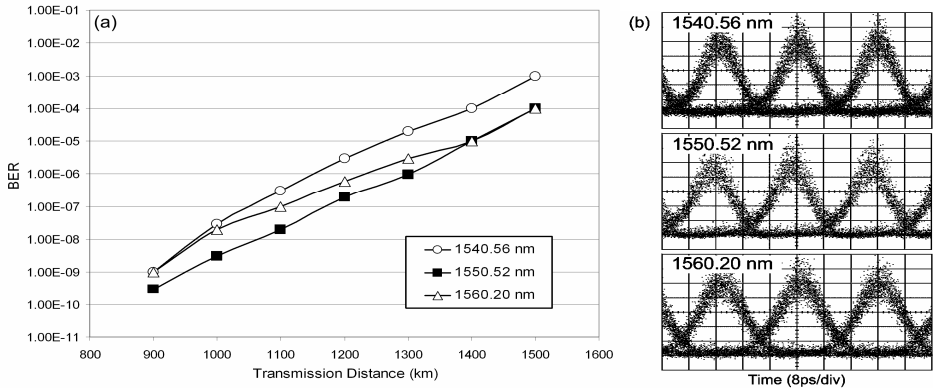

Fig. 7. (a). BER as a function of transmission distance for the optimized transmitter. (b). Corresponding eye diagrams received after 1000 km for 1540.56, 1550.52 and 1560.20 nm respectfully.

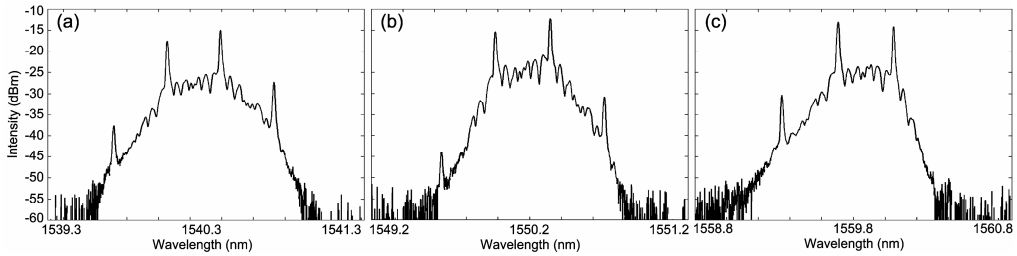

Fig. 8. Optical spectra for the three operating wavelengths, recorded after a transmission distance of 1000 km. (a) 1540.56 nm, (b) 1550.52 nm and (c) 1560.20 nm

4. Conclusion

We have presented the performance of a wavelength tunable pulse source, comprising of a SG DBR tunable laser and an EAM, in a 42.7 Gb/s re-circulating transmission system. It has been demonstrated that, in order to maintain a consistent level of performance and to achieve extended transmission reach over a wide wavelength range, it is imperative to tune the operating conditions of the EAM in the tunable transmitter. A linear spectrographic technique was employed to characterize the generated pulses in terms of pulse width, extinction ratio and chirp. This characterization provided an indication as to which EAM drive conditions would produce a pulse, which exhibits a chirp profile to match the residual dispersion experienced at each of three operating wavelengths in our transmission system. By optimizing the transmitter, near consistent transmission performance has been achieved at three different wavelengths spanning over a 20 nm range. Improvements of 150 and 400 km in transmission reach were achieved at operating wavelengths of 1550.52 and 1540.56 nm respectfully, relative to their non-optimized case. The optimized conditions for the tunable transmitter, obtained using the linear spectrogram characterization, could create a look up table, comprising of a RF drive voltage and a DC bias for each wavelength channel on the ITU grid. Therefore, as the SG DBR tunable laser is switched from one wavelength channel to another, the drive conditions of the EAM would be altered simultaneously to the corresponding optimum operating points for that wavelength, thereby achieving the ideal pulse profile for transmission, ensuring consistent performance is maintained over the entire waveband.

#95692 - $15.00 USD Received 1 May 2008; revised 19 Jun 2008; accepted 19 Jun 2008; published 11 Jul 2008